
Learning-Based Vulnerability Analysis of Cyber-Physical Systems

Amir Khazraei Spencer Hallyburton Qitong Gao Yu Wang Miroslav Pajic

Abstract

This work focuses on the use of deep learning for vulnerability analysis of cyber-physical systems (CPS). Specifically, we consider a control architecture widely used in CPS (e.g., robotics), where the low-level control is based on e.g., the extended Kalman filter (EKF) and an anomaly detector. To facilitate analyzing the impact potential sensing attacks could have, our objective is to develop learning-enabled attack generators capable of designing stealthy attacks that maximally degrade system operation. We show how such problem can be cast within a learning-based grey-box framework where parts of the runtime information are known to the attacker, and introduce two models based on feed-forward neural networks (FNN); both models are trained offline, using a cost function that combines the attack effects on the estimation error and the residual signal used for anomaly detection, so that the trained models are capable of recursively generating such effective sensor attacks in real-time. The effectiveness of the proposed methods is illustrated on several case studies.

1. Introduction

Although many cyber-physical systems (CPS) operate in safety-critical environments and the heterogeneous component connectivity provides numerous possible points of attack, most of the existing systems are only weakly protected by legacy components, such as fault/anomaly detectors. The challenge of securing CPS is even more

formidable due to the fact that the long system lifetime and resource constraints prevent the full use of new and existing security mechanisms. On the other hand, it has been recently shown that security-aware resource allocation can significantly reduce the security-related overhead and thus the cost of these systems (Lesi et al., 2017b; 2020; 2017a); the idea is to focus on protecting the critical system components and communication links, which if compromised could significantly degrade system performance. However, to achieve this, it is crucial to provide methods to analyze system vulnerability, in terms of performance degradation under attack, for different types of attacks and compromised components.

In this work, we investigate the use of deep learning for the vulnerability analysis of control mechanisms in CPS, focusing on attacks on system sensing. CPS controllers are commonly equipped with a state estimator that is used for low-level control as well as anomaly detection. Thus, attacks on sensing may have tremendous impact on the system (i.e., control performance). In such setting, to maximize the damage by exploiting the compromised components, the goal of the attacker is to perturb sensor measurements delivered to the controller such that the system is forced into an unsafe region, while the attack is undetected.

Consequently, a critical part of the vulnerability analysis is the design of effective and stealthy attack vectors; such attack generators should capture the impact that system dynamics has on both attack stealthiness and its effectiveness. There have been significant recent efforts focused on model-based design of stealthy attacks on CPS (Y. Mo and B. Sinopoli, 2010; Smith, 2015; Teixeira et al., 2012; Sui et al., 2020; Khazraei et al., 2017). However, these methods can be used only for linear dynamical systems, and thus have very limited applicability in practice.

The main difficulty in designing effective stealthy attacks for real-world systems with nonlinear dynamics is their complexity. To address this challenge, we employ deep learning to develop generators of such maximally effective yet stealthy attack signals (i.e., time series). Specifically, we propose two models for design of the attack vectors; each model requires different levels of runtime information from the state estimator (i.e., the current sensor measure-

This work is sponsored in part by the ONR under agreements N00014-17-1-2504 and N00014-20-1-2745, AFOSR under award number FA9550-19-1-0169, as well as the NSF CNS-1652544 award and the Intel-NSF partnership for cyber-physical systems security and privacy.

Authors are with the Department of Electrical and Computer Engineering, Duke University, Durham, NC 27708, USA. Emails: {amir.khazraei, spencer.hallyburton, qitong.gao, yu.wang094, miroslav.pajic}@duke.edu.

ments and the previous state estimation, or only the current sensor measurement). Both models are based on feed-forward neural networks (FNN) and trained offline such that the cost function captures the impact the attack would have on the estimation error and stealthiness requirements. Finally, we illustrate the use and evaluate effectiveness of our approach on case studies in the domain of autonomous driving and unmanned aerial vehicles (UAVs).

Note that this work is related in spirit to adversarial machine learning, which has recently attracted significant attention, studying methods to generate adversarial examples that could degrade performance of machine learning models (e.g., classifiers). For instance, by adding a small perturbation z to the input x , the attacker could design an adversarial example $x^* = x + z$ that results in miss-classification error $C(x^*) \neq C(x)$, for some classifier C (e.g., (Szegedy et al., 2013; Goodfellow et al., 2014; Papernot et al., 2017; Yuan et al., 2019)). The common assumption among such approaches (e.g., (Goodfellow et al., 2014; Kurakin et al., 2016; Moosavi-Dezfooli et al., 2016; Croce & Hein, 2020; Carlini & Wagner, 2017)) is that the predicted target only depends on its input (and not internal dynamics – i.e., previous states). On the other hand, to address requirements of attacking a system with internal dynamics, in this work, we consider models whose output should also depend on the previous outputs (i.e., previous state). In addition, both input and outputs belong to a continuous space.

To the best of our knowledge, this is the first study focused on the design of stealthy attack vectors (over time intervals) that degrade performance of state estimators, and thus the overall controllers, for nonlinear dynamical systems, and for which only limited knowledge of the physical model is available. Some recent works have considered adversarial machine learning beyond the image domain (Li et al., 2020; Zizzo et al., 2019; Feng et al., 2017). For example, (Li et al., 2020) studies vulnerability of machine learning models applied in CPS by proposing methods for generating adversarial examples that satisfy some physical constraints. However, unlike our work, the considered setup do not support or consider physical systems with dynamics.

1.1. Notation

We use \mathbb{R} to denote the set of real numbers, whereas \mathbb{P} and \mathbb{E} denote the probability and expectation for a random variable. For a matrix A , A^T denotes its transpose and for a square matrix $\text{trace}(A)$ denotes the trace of the matrix A . In addition, I is the identity matrix in general, while I_p denotes the identity matrix with dimension $p \times p$ (i.e., $I_p \in \mathbb{R}^{p \times p}$). Matrix $A \in \mathbb{R}^{n \times n}$ is positive semidefinite, which is denoted by $A \succeq 0$, if $x^T A x \geq 0$ holds for all $x \in \mathbb{R}^n$. For two positive semidefinite matrices A and B , we denote by $A \preceq B$ if it holds that $(B - A) \succeq 0$.

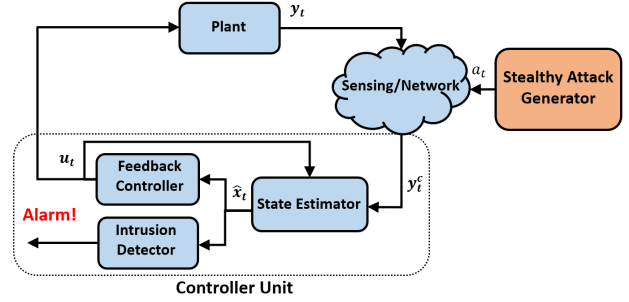


Figure 1. CPS Control architecture under attacks on system sensing – the considered general attack model captures the impact of both network-based attacks (e.g., man-in-the-middle attacks) and direct sensor attacks (e.g., sensor spoofing).

For a vector $x \in \mathbb{R}^n$, we denote by $\|x\|_p$ the p -norm of x ; when p is not specified, the 2-norm is implied. In addition, $\text{supp}(x)$ denotes the indices of the nonzero elements of $x \in \mathbb{R}^n$ – i.e., $\text{supp}(x) = \{i \mid i \in \{1, \dots, n\}, x_i \neq 0\}$. Finally, a function $h : \mathbb{R}^n \rightarrow \mathbb{R}^p$ is L -Lipschitz if for any $x, y \in \mathbb{R}^n$ it holds that $\|h(x) - h(y)\| \leq L\|x - y\|$.

2. Preliminaries and Problem Formulation

In this section, we formalize the problem considered in this work, starting from the security-aware system (i.e., including the attack) model. Specifically, we consider the setup from Fig. 1 with each component described in detail.

2.1. System Model

We consider a general nonlinear dynamical model of a physical system (i.e., plant) compromised by an attacker:

$$\begin{aligned} x_t &= f(x_{t-1}, u_{t-1}) + w_{t-1}, \\ y_t^c &= y_t + a_t = h(x_t) + v_t + a_t. \end{aligned} \quad (1)$$

Here, $x_t \in \mathbb{R}^n$ and $u_t \in \mathbb{R}^m$ denote the plant's state and input vectors at time t , whereas the output vector received by the controller $y_t^c \in \mathbb{R}^p$ contains the measurements from p sensors from the set $\mathcal{S} = \{s_1, \dots, s_p\}$, including compromised measurements provided by sensors from the set $\mathcal{K}_a \subseteq \mathcal{S}$; $a_t \in \mathbb{R}^p$ denotes the attack signal injected at time t , and thus the vector is sparse, with support in \mathcal{K}_a – i.e., $\text{supp}(a_t) = \mathcal{K}_a$ and $a_{t,i} = 0$ for $i \in \mathcal{K}_a^c$.¹ The observation function $h : \mathbb{R}^n \rightarrow \mathbb{R}^p$ is assumed to be L -Lipschitz. Finally, w_t and v_t are state and measurement noise.

In a special case, if the plant (1) is linear time-invariant (LTI), we use $f(x_t, u_t) = Ax_t + Bu_t$ and $h(x_t) = Cx_t$,

¹We refer to sensors from \mathcal{K}_a as compromised sensors, even if a sensor itself is not directly compromised, but its measurements may be altered due to e.g., network-based attacks. We may use \mathcal{K}_a to denote both the sets of compromised sensors and their indices.

where A , B and C are matrices of suitable dimensions.

Control Architecture. We consider a common control architecture, with three main components (Fig. 1): a state estimator, a feedback controller, and an anomaly detector.

The *State Estimator* (observer) employs the system model to predict its (state) evolution, and thus provide an estimate \hat{x}_t of its state at time t ; this can be in general captured as

$$\begin{aligned}\hat{x}_t &= O_t(\hat{x}_{t-1}, u_{t-1}, y_t), \\ \hat{y}_t &= h(\hat{x}_t).\end{aligned}\quad (2)$$

The mapping O_t is commonly designed such that (2) minimizes a norm of the estimation error defined as

$$\Delta x_t = x_t - \hat{x}_t. \quad (3)$$

Depending on the system model and statistical characteristics of the noise, different estimation methods are employed. Kalman filters are widely used for LTI systems, whereas Extended Kalman filters (EKFs) are mainly utilized in legacy (and new) nonlinear systems with Gaussian noise, e.g., the autonomous driving and UAV studies considered in this work. Thus, we particularly focus on EKFs.

The EKF functionality for a system from (1) is described by $\hat{x}_{t|t-1} = f(\hat{x}_{t-1}, u_{t-1})$, $\hat{x}_t = \hat{x}_{t|t-1} + L_t(y_t - h(\hat{x}_{t|t-1}))$, $\hat{y}_t = h(\hat{x}_t)$; (4)

here, $\hat{x}_{t|t-1}$, \hat{x}_t and \hat{y}_t denote the predicted state estimate, (updated) state estimate, and predicted output, respectively. The EKF gain L_t is also updated as

$$\begin{aligned}L_t &= A_t P_t C_t^T (C_t P_t C_t^T + R_t)^{-1}, \\ P_{t+1} &= A_t P_t A_t^T + Q_t - L_t (C_t P_t C_t^T + R_t) L_t^T,\end{aligned}\quad (5)$$

where $A_t = \frac{\partial f(x_t, u_t)}{\partial x_t} |_{\hat{x}_{t-1}, u_t}$ and $C_t = \frac{\partial h(x_t)}{\partial x_t} |_{\hat{x}_{t|t-1}}$ are the Taylor expansion of f and h around (\hat{x}_{t-1}, u_t) and $\hat{x}_{t|t-1}$, respectively. Furthermore, Q_t and R_t are the covariance matrix of the Gaussian noises w_t and v_t , respectively. Finally, the residue signal (or innovation noise) is defined as

$$z_t = y_t - h(\hat{x}_{t|t-1}). \quad (6)$$

For systems with Gaussian noise, its covariance matrix is $S_t = \mathbb{E}\{z_t z_t^T\} = C_t P_t C_t^T + R_t$ (Julier & Uhlmann, 2004).

The *Feedback Controller* employs the control law $u_t = \pi(\hat{x}_t)$, and without loss of generality, we assume the control goal is to regulate the states to $0 \in \mathbb{R}^n$. Therefore, the state estimator (2) can be modeled as

$$\hat{x}_t = O_t(\hat{x}_{t-1}, \pi(\hat{x}_{t-1}), y_t) \triangleq \mathcal{O}_t(\hat{x}_{t-1}, y_t). \quad (7)$$

The *Anomaly Detector* (AD) is used to detect the presence of system anomalies, including intrusions (i.e., attacks). The standard approach is to use the system model to predict the future system behavior and compare it with the actual

observation (e.g., see (Giraldo et al., 2018) and the references within); capturing the discrepancy between the system and its predicted behavior with a detection function g_t .

In feedback-control based CPS, the residue (6) is widely used for anomaly detection – χ^2 detector in (Y. Mo and B. Sinopoli, 2010; Mo & Sinopoli, 2015), cumulative sum in (Tunga et al., 2018), sequential probability ratio test (SPRT) detector in (Kwon et al., 2016), and a general window-type detector in (Jovanov & Pajic, 2019). For instance, with χ^2 -based detectors the detection function g_t is a weighted norm of z_t (with the χ^2 distribution) – i.e.,

$$g_t = z_t^T S_t^{-1} z_t; \quad (8)$$

the other detectors (e.g., from (Kwon et al., 2014; 2016; Mo & Sinopoli, 2015; Kwon & Hwang, 2017; Tunga et al., 2018; Y. Mo and B. Sinopoli, 2010; Miao et al., 2013; Miao et al., 2017; Jovanov & Pajic, 2019)) use some forms of a windowed extension of (8). Thus, to simplify our presentation, we focus on the detection function g_t from (8), and our results can be directly extended to other cases.

Finally, the system triggers alarm if the detection function satisfies that $g_t > \eta$, for some predefined threshold value η . Usually the value η is assigned such that under normal condition (i.e., when the system is not compromised) $\mathbb{P}(g_t > \eta) \leq \epsilon$ – i.e., the system has a low false alarm rate.

2.2. Attack Model

Attacker capabilities during offline training. Let T be the duration of the training phase; we define $\hat{X}_{t|t-1} = \{\hat{x}_{0|0}, \hat{x}_{1|0}, \dots, \hat{x}_{t|t-1}\}$, $Y_t = \{y_0, \dots, y_t\}$ and $\mathbf{L}_t = \{L_0, \dots, L_t\}$ as the sequences of the predicted states, plant outputs and EKF gains for $t \geq 0$, with 0 denoting the time starting the training phase. We assume that the attacker has access to the EKF values over time (either directly, or knowing the EKF design and running a copy of the EKF in parallel) – i.e., has access to $\hat{X}_{T|T-1}$, \mathbf{K}_T , Y_T and the function h . Meanwhile, for $0 \leq t < T$, the attacker can compromise the sensor measurements according to (1).

Attacker capabilities at runtime – during attack. Let t_0 denote the start time of the attack, modeled as in (1), and T' its duration. Again, we assume that the attacker has access to the sensor measurements y_t . In addition, we will consider two scenarios: when the attacker does (i.e., grey-) or does not (i.e., black-box) have access to the state estimation \hat{x}_{t-1} in the previous time step.

Attacker's goal is to *maximize degradation of control performance* – i.e., *Quality-of-Control* (QoC). Specifically, as only sensor data may be compromised, the attack objective is to *maximize the state estimation error* Δx_t . In addition, the attacker wants to *remain stealthy* – i.e., *undetected by the AD*. These notions are formalized as follows.

Definition 1. *The sequence of attack vectors $a_{t_0}, a_{t_0+1}, \dots$ is referred to as (ϵ, α) -successful if there exists $t' \geq t_0$ such that $\|\Delta x_{t'}\| \geq \alpha$ and $\mathbb{P}(g_t > \eta) \leq \epsilon$ for all $t \geq t_0$.²*

Therefore, the goal of the attacker is to insert a sequence of false data measurements $a_{t_0}, \dots, a_{t_0+T'}$ resulting in a (ϵ, α) -successful attack. Note that while Def. 1 focuses on attacks that result in a desired norm of the estimation error (i.e., $> \alpha$), for some systems, attacks may cause arbitrarily large estimation errors (Jovanov & Pajic, 2019). For LTI systems with (standard) Kalman filters, the notion of (ϵ, α) -successful attacks was first introduced in (Y. Mo and B. Sinopoli, 2010). Also, for LTI systems necessary and sufficient conditions such that (ϵ, α) -successful attacks exist for any $\alpha > 0$ are introduced in (Y. Mo and B. Sinopoli, 2010; Kwon et al., 2014; Jovanov & Pajic, 2019), along with a method to derive such attacks. However, to the best of our knowledge, there is no work that provides methods for vulnerability analysis of nonlinear systems (from (1)) under sensor-based attacks – i.e., the impact that such attacks would have on the estimation error, and thus QoC.

2.3. Vulnerability Analysis using Learning-Based Attack Design

Consequently, to evaluate impact that attacks on a subset of sensors \mathcal{K}_a might have on the system, we focus on learning-based attack design for nonlinear dynamical systems described in Sec. 2.1. Specifically, our goal is to develop learning based methods that for any nonlinear system (1), estimator (7), and desired $\alpha > 0$ and $\epsilon < 1$, derive an (ϵ, α) -successful attack sequence.

We start by building intuition about such attacks for LTI systems with Kalman filters, before using it to derive such attacks for nonlinear systems with EKF estimators. Then, we introduce a learning-based methodology to design such attacks for a general type of estimators from (7). To simplify our presentation, in the rest of this work we present the analysis when $\mathcal{K}_a = \mathcal{S}$; still, our methodology can be easily extended to $\mathcal{K}_a \subset \mathcal{S}$ as shown in the case studies.

3. Adversarial Learning for Nonlinear Dynamical Systems

We start with design methods for (ϵ, α) -successful attacks against LTI systems with standard Kalman filters.

Lemma 1 ((Y. Mo and B. Sinopoli, 2010; Kwon et al., 2014; Jovanov & Pajic, 2019)). *For an LTI system with a Kalman filter-based estimator, there exist (ϵ, α) -successful attacks for any desired $\alpha > 0$ if and only if the matrix A is unstable and at least one eigenvector v corresponding to*

²Any p -norm can be used; in this work, when p is not specified, the 2-norm is implied.

an unstable eigenvalue satisfies that $\text{supp}(Cv) \subseteq \mathcal{K}_a$.

Therefore, matrix A being unstable is a necessary condition for LTI systems with Kalman filters to be (ϵ, α) -successful attack for arbitrarily large α . However, if all sensors are under attack (i.e., $\mathcal{K}_a = \mathcal{S}$, as considered here), this is also a sufficient condition. A similar necessary and sufficient condition for LTI systems with attack-resilient estimators (e.g., from (Fawzi et al., 2014; Pajic et al., 2017b;a)) is derived in (Khazraei & Pajic, 2020).

In the following theorem, we show how to use only the current state estimation \hat{x}_t and the plant output y_t to compute such attack sequence for arbitrarily large α .

Theorem 1. *Consider an LTI system with unstable matrix A , and let ϕ_t denote a Gaussian noise vector satisfying $\mathbb{E}\{\phi_t\} = 0$ and $\mathbb{E}\{\phi_t \phi_t^T\} \preceq S$. The attack sequence generated by $a_t = -y_t + CBu_{t-1} + CA\hat{x}_{t-1} + \phi_t$, for $t \geq 0$, is an (ϵ, α) -successful attack for any arbitrary $\alpha > 0$.*

Proof. First, we will show that applying such attack sequence results in an unbounded estimation error. For LTI systems, the dynamic of the state estimation error follows

$$\begin{aligned} \Delta x_t &= x_t - \hat{x}_t \\ &= A\Delta x_{t-1} + w_t - L(y_t^c - CA\hat{x}_{t-1} - CBu_{t-1}) \\ &= A\Delta x_{t-1} + w_t - L\phi_t \end{aligned}$$

As the matrix A is unstable, it follows that $\|\Delta x_t\|$ will be unbounded as $t \rightarrow \infty$.

We now show that the attack is stealthy from the perspective of the IDS. In this case, the residue signal z_t satisfies

$$\begin{aligned} z_t &= y_t^c - C(A\hat{x}_{t-1} + Bu_{t-1}) \\ &= y_t + a_t - C(A\hat{x}_{t-1} + Bu_{t-1}) = \phi_t. \end{aligned} \quad (9)$$

Therefore, it follows that

$$\begin{aligned} \mathbb{E}\{g_t^a\} &= \mathbb{E}\{z_t^T S^{-1} z_t\} = \mathbb{E}\{\phi_t^T S^{-1} \phi_t\} \\ &= \text{trace}(\mathbb{E}\{\phi_t^T S^{-1} \phi_t\}) = \mathbb{E}\{\text{trace}(\phi_t \phi_t^T S^{-1})\} \\ &= \text{trace}(\mathbb{E}\{\phi_t \phi_t^T\} S^{-1}) \leq \text{trace}(SS^{-1}) = p, \end{aligned}$$

where we used the linearity of expectation and trace operation. Note that for LTI systems, the expectation of g_t (also known as the degrees of freedom of the distribution) satisfies that $\mathbb{E}\{g_t\} = p$. Based on the properties of the χ^2 distribution, since $\mathbb{E}\{g_t^a\} \leq \mathbb{E}\{g_t\} = p$, it follows that $\mathbb{P}(g_t^a > \eta) \leq \mathbb{P}(g_t > \eta) = \epsilon$, and thus the attack sequence is stealthy. \square

Consequently, unlike the design of adversarial examples for images (e.g., (Szegedy et al., 2013; Goodfellow et al., 2014; Papernot et al., 2017; Yuan et al., 2019)), for LTI dynamical systems, an effective and stealthy attack sequence has to evolve over time (i.e., following suitable dynamics). This

inspires us to use a similar structure for generating effective stealthy attacks against nonlinear dynamical systems. Specifically, inspired by Theorem 1, we consider attack with dynamics $a_t = F(\hat{x}_{t-1}, y_t)$ (since y_t and \hat{x}_{t-1} are both functions of a_{t-1}), with the idea to use a deep feed-forward neural network (FNN) to learn F . However, the attacker might not always have access to \hat{x}_{t-1} during the attack. Thus, we will consider both the cases where \hat{x}_{t-1} is available and when it is not. For the latter, the idea is to replace \hat{x}_t with another signal r_t that is directly constructed by the attacker. In what follows, we summarize two proposed models to design (ϵ, α) -successful attack vectors.

FNN-based attack design. When \hat{x}_{t-1} is available to the attacker, we design an FNN that uses the current output measurements and the last state estimation to generate the next attack vector – i.e.,

$$a_t = H_\theta(y_t, \hat{x}_{t-1}), \quad (10)$$

where H_θ is a deep FNN with parameters θ with input dimension of $n + p$ and output dimension p .

delayed FNN (dFNN)-based attack design. When \hat{x}_{t-1} is not available to the attacker, we consider an architecture, referred to as dFNN, that uses only the current sensor measurements for attack design as follows

$$\begin{aligned} r_t &= G_\theta(y_t, r_{t-1}), \\ a_t &= W r_t; \end{aligned} \quad (11)$$

here, G_θ is a deep FNN with parameters θ , while $W \in \mathbb{R}^{l \times p}$ is a linear mapping from the state r_t to the attack vector a_t . Intuitively, $r_t \in \mathbb{R}^l$ and G_θ should allow for capturing of the evolution of \hat{x}_t , to create a dynamical pattern for the sequence of attack vectors in the dFNN design (11). Note that effectively (11) captures a simplified version of the standard recurrent neural networks (RNN) but without the full feedback between all the network layers.

Model training. To capture the attack impact on the estimation error, the first challenge lies in the fact that the actual true state of the plant x_t is not available to the attacker; rather only sensor measurements y_t are known. Thus, we start with a result showing that under some mild assumptions, the sensor measurements can be directly used.

Theorem 2. *If the function $h : \mathbb{R}^n \rightarrow \mathbb{R}^p$ is Lipschitz with constant L , then $\|y_t - h(\hat{x}_t)\| \geq \alpha$ implies $\|x_t - \hat{x}_t\| \geq \frac{\alpha - \sqrt{\sigma k}}{L}$ with probability $1 - \frac{p}{k^2}$, for $k < \frac{\alpha}{\sigma}$ and $R \preceq \sigma I$; here, I is the identity matrix and σ is a positive scalar.*

Proof. From the multivariate Chebyshev's inequality (Navarro, 2016), it holds that $\mathbb{P}(v_t^T R^{-1} v_t \leq k^2) \geq 1 - \frac{p}{k^2}$. On the other hand, using our assumption $R \preceq \sigma I$, it holds that $\sigma^{-1} v_t^T v_t \leq v_t^T R^{-1} v_t$ for any $v_t \in \mathbb{R}^p$. Therefore, $\mathbb{P}(v_t^T v_t \leq \sigma k^2) \geq 1 - \frac{p}{k^2}$ or equivalently $\mathbb{P}(\|v_t\| \leq$

$\sqrt{\sigma k}) \geq 1 - \frac{p}{k^2}$. Now, with the probability of at least $1 - \frac{p}{k^2}$, we have that

$$\begin{aligned} \alpha &\leq \|y_t - h(\hat{x}_t)\| = \|h(x_t) + v_t - h(\hat{x}_t)\| \leq \\ &\leq L\|x_t - \hat{x}_t\| + \|v_t\| \leq L\|x_t - \hat{x}_t\| + \sqrt{\sigma k}, \end{aligned}$$

which results in $\|x_t - \hat{x}_t\| \geq \frac{\alpha - \sqrt{\sigma k}}{L}$. \square

We use $a_t = F_\Theta(y_t, s_{t-1})$ to capture the attack vectors generated by either (10) or (11) (e.g., s_t indicates either r_t or \hat{x}_t). Our goal is to train the parameters in (10) and (11) so that (10) and (11) act as generators of (ϵ, α) -successful attacks. Specifically, the generated attack vectors starting from t_0 , should at some $t' > t_0$ result in $\|x_{t'} - \hat{x}_{t'}\| \geq \alpha$, while $\mathbb{P}(g_t > \eta) \leq \epsilon$ for $t \geq t_0$ for all $t_0 \leq t \leq t'$.

Thus, by starting training at time 0 we are seeking for a_0 that maximizes $\|x_0 - \hat{x}_0^a\|$ with $\hat{x}_0^a = \mathcal{O}(\hat{x}_{-1}, y_0^c)$ and $y_0^c = y_0 + a_0$. As the true state x_0 is not available, from Theorem 2, we can maximize $\|y_0 - h(\hat{x}_0^a)\|$ instead. Also, the generated attack should satisfy the stealthiness condition $\mathbb{P}(g_0^a > \eta) \leq \epsilon$ with $g_0 = \|y_0^c - \hat{y}_0\|^2$ (note that for χ^2 -based ADs, it holds that $\hat{y}_0 = h(\hat{x}_{0|-1})$). Therefore, the following optimization problem should be solved at time 0:

$$\begin{aligned} \max_{\Theta} & \|y_0 - h(\hat{x}_0^a)\| \\ \text{s.t.} & \mathbb{P}(g_0^a > \eta) \leq \epsilon \\ & a_0 = F_\Theta(y_0, s_{-1}). \end{aligned}$$

As this constrained optimization problem is challenging to solve, we penalize the norm of the residue signal and incorporate a new term in our objective function – i.e., the following optimization problem is considered:

$$\begin{aligned} \min_{\Theta} & g_0^a - \delta \|y_0 - h(\hat{x}_0^a)\| \\ & a_0 = F_\Theta(y_0, s_{-1}); \end{aligned} \quad (12)$$

here, $\delta > 0$ is a standard regularization term balancing the stealthiness condition and performance degradation caused by the estimation error.

Let us denote the parameters obtained from (12) as $\Theta^{(0)}$. Now, the attack vector $a_0 = F_{\Theta^{(0)}}(y_0, s_0)$ applied to the sensor measurements at time 0, would result in state estimate $\hat{x}_0^a = \mathcal{O}(\hat{x}_{-1}, y_0^c)$. In the next time step, we want to find the parameters such that $g_1^a - \delta \|y_1 - h(\hat{x}_1^a)\|$ is minimized. However, in this case the parameters will only be trained to minimize the cost function at time 1 and thus will disregard minimization of the cost function in the previous time step. Hence, the cost function from the previous time step should be also included – i.e., the objective function to be minimized at time 1 should be $g_0^a + g_{t_0+1}^a - \delta (\|y_0 - h(\hat{x}_0^a)\| - \|y_1 - h(\hat{x}_1^a)\|)$.

This approach should continue for the following time steps. Generally, if we consider that the training starts at 0, for

Algorithm 1 Stealthy Attack Synthesis Using FNN

```

1: Set the learning rate  $\beta$  and training period  $T'$ 
2: for  $t = 0 : T'$  do
3:    $x_t = f(x_{t-1}, u_{t-1}) + w_{t-1}$ 
4:    $y_t = h(x_t) + v_t$ 
5:    $\hat{x}_{t|t-1} = f(\hat{x}_{t-1}, u_{t-1})$ 
6:   repeat
7:      $J'_t = \lambda_t \sum_{j=0}^{t-1} J_j + J_t$  with  $y_j^c = y_j + H_\theta(\hat{x}_{j-1}, y_j)$ 
8:      $\theta^{(t)} \leftarrow \theta^{(t)} - \beta \nabla_{\theta} J'_t$ 
9:   until Convergence
10:   $a_t = F_{\theta^{(t)}}(\hat{x}_{j-1}, y_j)$ 
11:   $y_t^c = y_t + a_t$ 
12:   $\hat{x}_t = \hat{x}_{t|t-1} + L_t(y_t^c - h(\hat{x}_{t|t-1}))$ 
13: end for
    
```

any $t \geq 0$ there should be an instantaneous cost function defined by $J_t = g_t^a - \delta \|y_t - h(\hat{x}_t^a)\|$. Therefore, the optimization problem that is solved at time step t is

$$\min_{\Theta} J_t + \lambda_t \left(\sum_{j=0}^{t-1} J_j \right) \quad (13)$$

$$a_t = F_{\Theta}(y_t, s_{t-1}).$$

Again, $\lambda_t \geq 0$ are regularization terms to control the incorporation of previous cost functions. If $\lambda_t = 1$, we effectively penalize all previous and current instantaneous costs equally. For smaller values of λ_t , the cost function at time t will be approximately J_t – i.e., we can do more exploration by only minimizing the cost at time t . However, increasing λ_t helps exploit more by giving more importance to the previous cost functions.

Finally, once the model parameters are obtained from (13), the attack vector $a_t = F_{\Theta^{(t)}}(y_t, s_{t-1})$ is applied to the system, and the process is repeated until the training completes. For the case when the estimator \mathcal{O} is the EKF, Algorithms 1 and 2 provide pseudocode for learning the attack generators for the FNN and dFNN-based models.

4. Case Studies

We illustrate and evaluate our attack-design framework on two realistic case studies, autonomous driving vehicles (ADV) and unmanned aerial vehicles (UAV).

4.1. Autonomous Driving Vehicles

Generic Vehicle Model. We first considered a simple nonlinear dynamical model of ADV from (Kong et al., 2015), with four states $[x \ y \ \psi \ v]^T$; here, x and y represent the position of the center of mass in x and y axis, respectively, ψ is the inertial heading, and v is the velocity of the vehicle. We assume that two states $[x \ y]^T$ are measured using sensors, however, the measurements are

Algorithm 2 Stealthy Attack Synthesis Using dFNN

```

1: Set the learning rate  $\beta$  and training period  $T'$ 
2: for  $t = 0 : T'$  do
3:    $x_t = f(x_{t-1}, u_{t-1}) + w_{t-1}$ 
4:    $y_t = h(x_t) + v_t$ 
5:    $\hat{x}_{t|t-1} = f(\hat{x}_{t-1}, u_{t-1})$ 
6:   repeat
7:      $J'_t = \lambda_t \sum_{j=0}^{t-1} J_j + J_t$  with  $y_j^c = y_j + WG_\theta(r_{j-1}, y_j)$ 
8:      $\theta^{(t)} \leftarrow \theta^{(t)} - \beta \nabla_{\theta} J'_t$ 
9:      $W^{(t)} \leftarrow W^{(t)} - \beta \nabla_W J'_t$ 
10:  until Convergence
11:   $r_t = G_{\theta^{(t)}}(r_{t-1}, y_t)$ 
12:   $a_t = W^{(t)} r_t$ 
13:   $y_t^c = y_t + a_t$ 
14:   $\hat{x}_t = \hat{x}_{t|t-1} + L_t(y_t^c - h(\hat{x}_{t|t-1}))$ 
15: end for
    
```

affected by noise with zero mean and covariance matrix $R = \text{diag}(.01, .01)$. The system noise is also zero mean, with covariance matrix $Q = .001I$.

We consider two different tasks for evaluating our attack generators. The first task is when the car is driven on a straight road with a constant speed of $10m/s$. The second task is driving the car with a constant speed of $10m/s$ on a curvy road. For both tasks, a feedback control law is used to keep the car between the lanes. We used Algorithms 1 and 2 to train the FNN and dFNN models for generating stealthy attacks. The network G_θ is a fully connected $5 \times 15 \times 15 \times 3$ network with ReLU activation function followed by $W \in \mathbb{R}^{3 \times 2}$. The network H_θ is also a fully connected $5 \times 15 \times 15 \times 2$ network with ReLU activation function. We trained the considered network for $T = 1000$ time steps, with $\delta = .2$ and $\lambda = .05$ for both tasks.

Fig. 2a shows the trajectory of the car driving on the straight road. Before starting the attack at the location $X = 100m$, the car (blue line) is moving between the lanes and the estimated trajectory (green line) has a very small estimation error. However, using either attacks derived by the FNN or dFNN-based attack generators, the car is being pushed off the road while the estimated position shows that the car is still in the road. Furthermore, the attacks are stealthy – the anomaly detector cannot detect the presence of either of the attacks. Fig. 2b and Fig. 2c illustrate the estimation error along the X and Y axis for these scenarios. Although the both models are trained offline for 1000 time steps, they can render stealthy attack for a longer time period, even more than 3000 time steps.

Fig. 3a and 3b show the trajectory of the car in the second scenario, driving on a curvy road, where non-linearity of the vehicle dynamics is highlighted. Before the attack

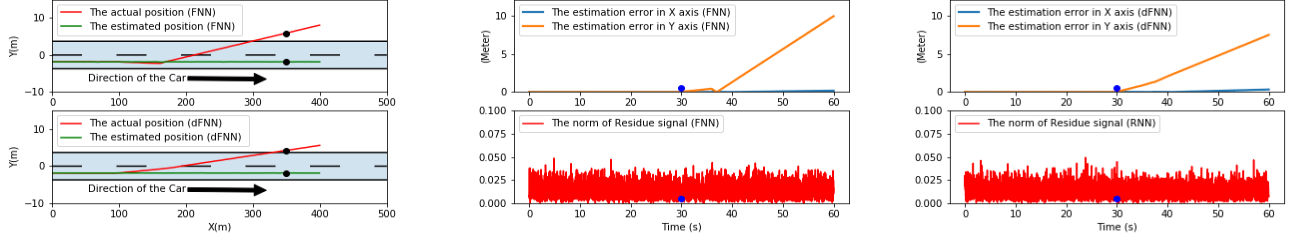


Figure 2. (a) The trajectory of the compromised car on the road using both models of FNN and RNN. The green line is the estimated position and the red line is the actual position of the car. The red dot shows the place where the attacker starts attacking the system. The black dots also show the actual and estimated position of the car at the same time. (b,c) The above sub-figures show the state estimation error in x and y axis. The below sub-figures illustrate the norm of residue signal before and after the start time of attack $t = 30s$ (the blue dots) for each FNN and RNN methods.

starts at origin $X = 0, Y = 0$, the actual position of the car (red line) is between the lanes and the estimated trajectory (green line) has a very small estimation error. Using both FNN and dFNN-based attack generators, after the attacks start, the car gradually deviates from its original path and goes off the road. However, the estimated position shows that the car is still between the road lanes. The lower sub-figures in Fig. 3c and Fig. 3d show that the norm of the residue signal for the same experiments $-g_t$ does not change much after the start point of the attack at $t = 15s$, and thus, the anomaly detector did not detect the attack in both cases. Fig. 3c and Fig. 3d also present the estimation errors along the X and Y axis. For both FNN and dFNN-based attack generators, the estimation error along X and Y axis increases gradually.

Real-World Autonomous Driving Simulator – Evaluating on CARLA. To evaluate our methodology on very complex, realistic systems, for which we do not know the model of the highly non-linear vehicle dynamics, we evaluated our framework on ADV scenarios designed using the open-source vehicle simulator CARLA (Dosovitskiy et al., 2017). CARLA is an urban driving simulator built on Unreal Engine 4, providing realistic physics and sensor models in complex urban environments with static and dynamic actors.

We define a planning-navigation-control loop that drives the autonomous agent in our CARLA experiments. For planning, CARLA provides with a state-machine waypoint following algorithm. A vehicle’s (estimated) pose and velocity are used along with map-based waypoints to coordinate (i) road-following, (ii) left-turn, (iii) right-turn, (iv) intersection, and (v) hazard-stop conditions (Dosovitskiy et al., 2017). We estimate the pose and velocity using an EKF with high-rate sensor data.

We also leverage the EKF structure to design an industry-standard chi-square anomaly detector. As sensor inputs,

a Global Navigation Satellite Sensor (GNSS) sensor provides loosely coupled position solutions in global coordinates, a commercial GNSS standard. We similarly define a generalized velocimeter model, derived from Doppler (or, more frequently in safety-critical applications, GNSS delta-range). To simplify our presentation, we assume no discrepancy between time-of-arrival and time-of-validity in sensor measurements.

State estimates and planning objectives are feed into a standard feedback controller (Emirler et al., 2014) that targets a cruising speed of 25 km/hr ($\sim 7m/s$). The control algorithm drives the following actuators with associated input ranges: (i) Steering wheel angle on $[-1.0, 1.0]$, (ii) Throttle on $[0.0, 1.0]$, and (iii) Brake on $[0.0, 1.0]$. Finally, we visualize the vehicle trajectory and system integrity with a heads-up-display presented in Fig. 4 – the full-length videos for our CARLA experiments are available at (CPSL@Duke, 2021).

We use CARLA to evaluate our FNN and dFNN attack-generators for performance and generalizability. We also compare to the nominal case, i.e., without attacks. We showcase model performance by illustrating how both FNN and dFNN-based attack generators are able to drive the vehicle into unsafe situations (e.g., crashes into other cars or static objects) over short times while remaining undetected by the system anomaly detector.

During training and testing in the CARLA simulations, the GNSS and velocimeter both provide measurements to the navigation filter. However, to highlight the evaluation when not all of the sensors are compromised (i.e., $\mathcal{K}_a \neq \mathcal{S}$), we will focus our presentation here to the scenarios where the FNN and dFNN-based attack generator *are only be able to attack GNSS position measurements and to only have knowledge of positions states* (i.e., no knowledge of velocity or heading). Despite these restrictions on considered attacks, both the FNN and dFNN-based attack generators were able to produce attack vectors suitable of significantly

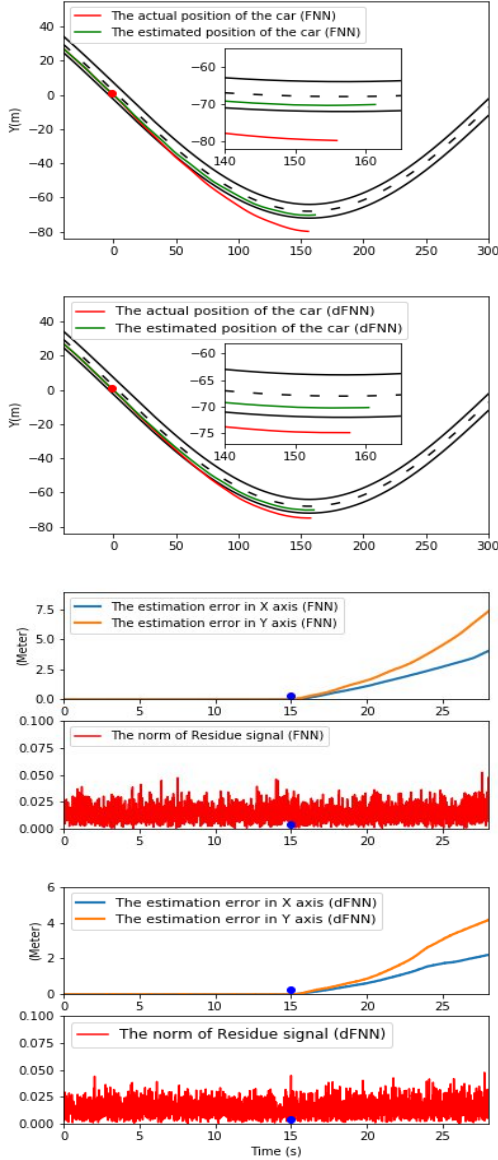


Figure 3. (a,b) The trajectory of the compromised car on a curly road. The green line shows the estimated position and red line shows the actual position of the car for each of the figures. The red dot shows the place where the attack starts on the system. (c,d) The above sub-figure shows the state estimation error in x and y axis. The below sub-figure illustrates the norm of residue signal before and after the start time of attack $t = 15s$.

moving the vehicle off-course without being detected – i.e., even a simple attack with imperfect information can be capable of disrupting a more complex system (e.g., resulting in a traffic incident).

Additionally, we demonstrate the attack generalizability twofold. First, we train the FNN and dFNN-based models off-line on a simple path (i.e., not the testing path) us-

ing only a state estimator without planning or control. The simple training path defines the car as a point-mass traveling straight at constant velocity with no forces acting upon the vehicle, no physics calculations, and no environment to interact with. We then test those same models on the full CARLA environment and path with all modules implemented. Second, we demonstrate the proof-of-concept that our attack models are able to generalize to different rates of sensor data by training at 100 Hz measurements and testing at 120 Hz measurements and retaining attack stealthiness and effectiveness.

Fig. 4 presents some of the results. Specifically, Fig. 4d shows the path and residue values when the sensors are NOT under attack. Fig. 4e and Fig. 4f show the path and the residue signal values of the compromised car when the FNN and dFNN-based generators are used to create inserted attack signals. The endpoint of the path is when the car hits an object and stops moving. Note that the residue signal has a huge spike only when the car hits the object (due to the collision), too late for any recovery action.

4.2. Unmanned Aerial Vehicles

Finally, we consider a quadrotor with nonlinear model from (Bouabdallah & Siegwart, 2007) which has twelve states $[x, y, z, \psi, \theta, \phi, \dot{x}, \dot{y}, \dot{z}, \dot{\psi}, \dot{\theta}, \dot{\phi}]^T$; x, y and z represent the quadrotor position along the X, Y and Z axis, respectively, while \dot{x}, \dot{y} and \dot{z} are their velocity. ψ, θ and ϕ are yaw, pitch and roll angles respectively and $\dot{\psi}, \dot{\theta}$ and $\dot{\phi}$ represent their corresponding angular velocity. The system is sampled using Euler method with $T_s = .05s$. It is assumed that the states $[x, y, z, \psi, \theta, \phi, \dot{\psi}, \dot{\theta}, \dot{\phi}]^T$ are measured and are affected by zero-mean Gaussian noise with the covariance matrix $R = .05I$. The system noise is also zero mean Gaussian with the covariance matrix $Q = .001I$.

Similar to the ADV case study, we consider two different tasks. First, we consider altitude control (Bouabdallah & Siegwart, 2007), where the drone should reach a predefined height (20m) and stay there (i.e., stay at coordinates $X = 0, Y = 0$ and $Z = 20$ if the initial point is denoted as $(0, 0, 0)$). For the second task we consider the trajectory tracking problem where the goal is to keep the drone in $X = 0, Y = 0$ position, while tracking the height $Z(t) = .2t$, for $t \geq 0$. UAV control for these two tasks is based on a standard feedback-based controller.

G_θ used for synthesizing the stealthy attack is a fully connected $29 \times 50 \times 100 \times 100 \times 100 \times 20$ network with ReLU activation function and $W \in \mathbb{R}^{20 \times 9}$ is the linear mapping. H_θ is also a fully connected $21 \times 50 \times 100 \times 100 \times 100 \times 9$ network with ReLU activation function. We found that $\lambda = .05$ in (13) results in the best performance for both models. After training the network for $T = 4500$ time

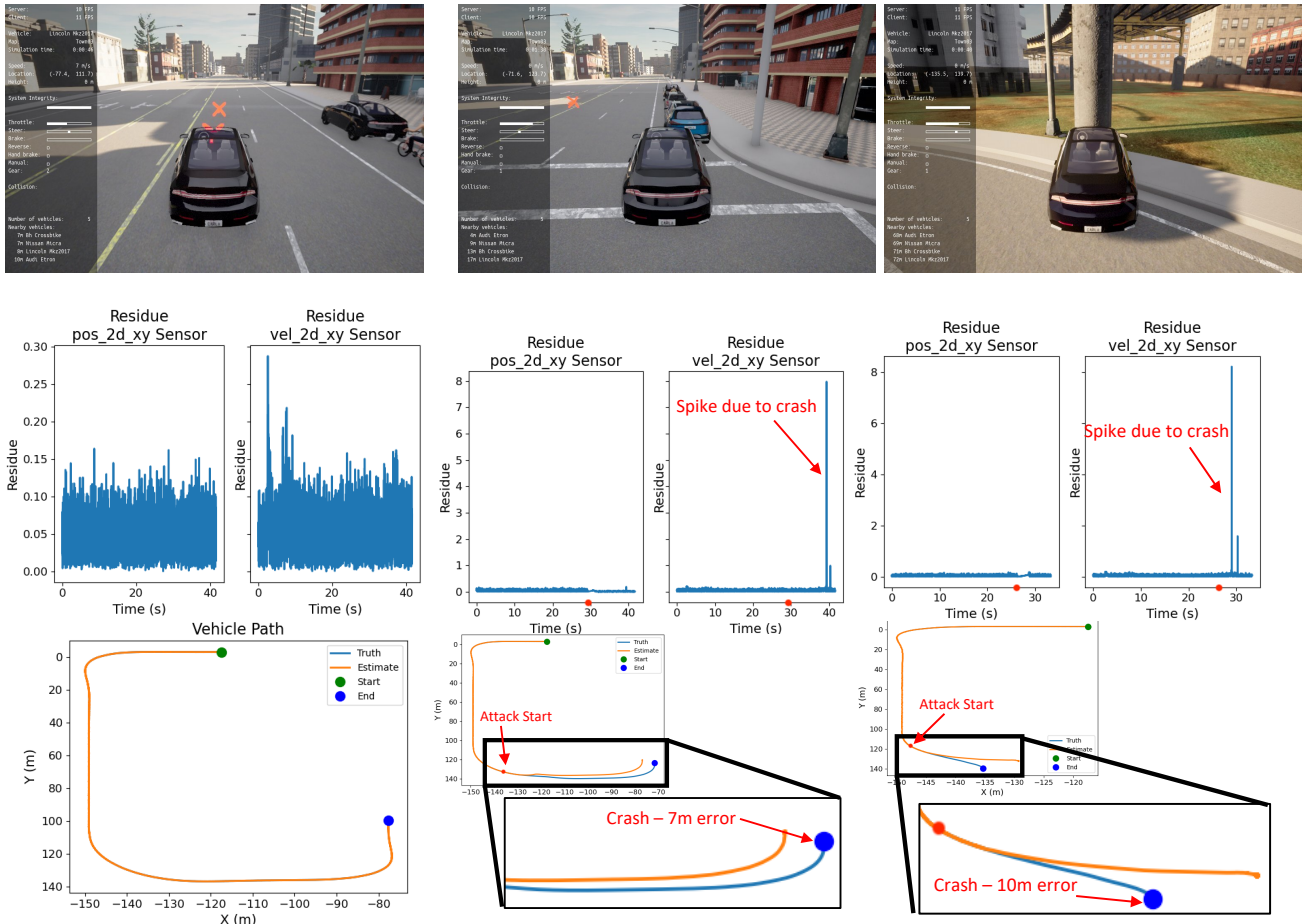


Figure 4. (a) The car in CARLA simulation environment tracking the center of the road using feedback controller when the system is free of attack; (b,c) The collision of the car with off the road objects due to the injecting sensor attacks using the FNN and dFNN-based attack generators, respectively; (d) The vehicle trajectory without attack and the residue signal for both velocity and position sensors; (e,f) The vehicle trajectory when the position sensors are compromised using the FNN and dFNN-based methods, respectively, and the corresponding residue signals.

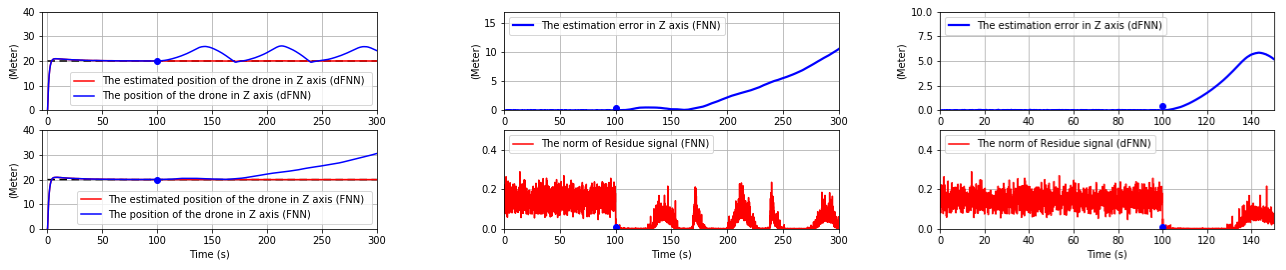


Figure 5. UAV altitude control: (a) The actual and estimated height of the drone for d-FNN and FNN-based attack (the blue dot highlights where the attacks starts); (b,c) The error of the estimated height (top) and the residue signal (bottom) for the FNN and dFNN-based attacks, respectively.

steps according to Algorithms 1 and 2, we used the obtained attack generators to synthesize UAV sensor attacks. Fig. 5a shows the UAV height (i.e., Z axis) over time,

for the altitude control scenario. Before the attack starts at $t = 100s$, the UAV moves from the ground ($Z = 0$) to the desired height $Z = 20m$. After the attacks start, the UAV deviates from the desired height for both attack

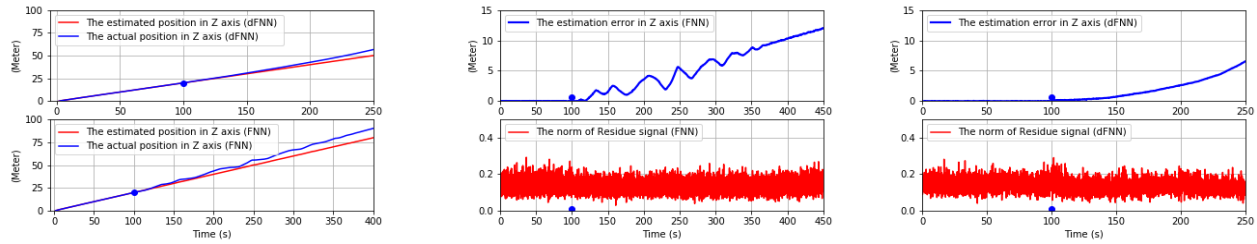


Figure 6. UAV trajectory control: (a) The actual and estimated UAV height for d-FNN and FNN-based attack (the blue dot highlights where the attacks starts); (b,c) The error of the height estimation (top) and the residue signal (bottom) for the FNN and dFNN-based attacks, respectively.

models (FNN and dFNN). On the other hand, the estimator perceives that the UAV is still at the desired height, while the residues is below the triggering threshold – i.e., the attacks are stealthy. Specifically, Fig. 5b and Fig. 5c show the estimator outputs. Both attack models were trained to reach $\alpha = 5m$ error while remaining stealthy. The FNN attack model causes almost $10m$ estimation error compared to dFNN-based attacks with $6m$ estimation error.

Fig. 6a presents the height of the UAV over time, for the trajectory control scenario. Before the attack starts at $t = 100s$, the UAV successfully tracks the height trajectory $Z = .2t$ for $0 \leq t \leq 100$. When the attack starts at time $t = 100s$, for both attack generators the actual (true) position deviates from the desired position while the estimated position falsely show that the UAV is still tracking the desired trajectory. Specifically, Fig. 6b and Fig. 6c show the error of the estimated height, for FNN- and dFNN-based attack generators, trained for $\alpha = 5m$. The FNN-based generator again outperforms as it causes almost $12m$ of error compared to the $6m$ for the dFNN-based attack generator, while both attacks remain stealthy with the residue signal below the alarm threshold.

5. Conclusion

In this work, we have utilized deep learning to generate stealthy attacks on control components in cyber-physical systems, focusing on a widely used architecture where the low-level control is based on the extended Kalman filter and an anomaly detector. We have considered a grey box setup, with unknown nonlinear plant dynamics and known observation functions and Kalman filter gains. We have shown that feedforward and delayed feedforward neural networks (FNN and dFNN, respectively) can be used to generate stealthy adversarial attacks on sensing information delivered to the system, resulting in large errors to the estimates of the state of the system without being detected.

Both FNN and dFNN are trained offline from a cost function combining the attack effects on the estimation error and the residual signal of the EKF; thus, the trained model

is capable of recursively generating such effective sensor attacks in real-time using only current sensor measurements. We have observed that the FNN-based model, due to having access to the current information of the system (output and state estimates), is more effective than dFNN, where a latent variable needs to capture the dynamics. The effectiveness of the proposed methods has been illustrated and evaluated on several case studies, with varying complexity, focused on Autonomous Driving Vehicles (specifically using complex scenarios in CARLA simulation environment) and Unmanned Aerial Vehicles (UAV).

References

- Bouabdallah, S. and Siegwart, R. Full control of a quadrotor. In *2007 IEEE/RSJ International Conference on Intelligent Robots and Systems*, pp. 153–158. Ieee, 2007.
- Carlini, N. and Wagner, D. Towards evaluating the robustness of neural networks. In *2017 IEEE Symposium on Security and Privacy (SP)*, pp. 39–57. IEEE, 2017.
- CPSL@Duke. Vulnerability Analysis of Autonomous Vehicles. <https://cpsl.pratt.duke.edu/research/vulnerability-autonomous-vehicles>, 2021.
- Croce, F. and Hein, M. Minimally distorted adversarial examples with a fast adaptive boundary attack. In *International Conference on Machine Learning*, pp. 2196–2205. PMLR, 2020.
- Dosovitskiy, A., Ros, G., Codevilla, F., Lopez, A., and Koltun, V. Carla: An open urban driving simulator. In *Conference on robot learning*, pp. 1–16. PMLR, 2017.
- Emirler, M. T., Uygan, İ. M. C., Aksun Güvenç, B., and Güvenç, L. Robust pid steering control in parameter space for highly automated driving. *International Journal of Vehicular Technology*, 2014, 2014.
- Fawzi, H., Tabuada, P., and Diggavi, S. Secure estimation and control for cyber-physical systems under adversarial

- attacks. *IEEE Transactions on Automatic control*, 59(6): 1454–1467, 2014.
- Feng, C., Li, T., Zhu, Z., and Chana, D. A Deep Learning-based Framework for Conducting Stealthy Attacks in Industrial Control Systems. *arXiv:1709.06397 [cs]*, 2017.
- Giraldo, J., Urbina, D., Cardenas, A., Valente, J., Faisal, M., Ruths, J., Tippenhauer, N. O., Sandberg, H., and Candell, R. A survey of physics-based attack detection in cyber-physical systems. *ACM Computing Surveys (CSUR)*, 51(4):1–36, 2018.
- Goodfellow, I. J., Shlens, J., and Szegedy, C. Explaining and harnessing adversarial examples. *arXiv preprint arXiv:1412.6572*, 2014.
- Jovanov, I. and Pajic, M. Relaxing integrity requirements for attack-resilient cyber-physical systems. *IEEE Transactions on Automatic Control*, 64(12):4843–4858, Dec 2019. ISSN 2334-3303. doi: 10.1109/TAC.2019.2898510.
- Julier, S. J. and Uhlmann, J. K. Unscented filtering and nonlinear estimation. *Proceedings of the IEEE*, 92(3): 401–422, 2004.
- Khazraei, A. and Pajic, M. Perfect attackability of linear dynamical systems with bounded noise. In *2020 American Control Conference (ACC)*, pp. 749–754, 2020.
- Khazraei, A., Kebriaei, H., and Salmasi, F. R. A new watermarking approach for replay attack detection in lqg systems. In *56th IEEE Annual Conf. on Decision and Control (CDC)*, pp. 5143–5148, 2017.
- Kong, J., Pfeiffer, M., Schildbach, G., and Borrelli, F. Kinematic and dynamic vehicle models for autonomous driving control design. In *2015 IEEE Intelligent Vehicles Symposium (IV)*, pp. 1094–1099. IEEE, 2015.
- Kurakin, A., Goodfellow, I., and Bengio, S. Adversarial examples in the physical world. *arXiv preprint arXiv:1607.02533*, 2016.
- Kwon, C. and Hwang, I. Reachability analysis for safety assurance of cyber-physical systems against cyber attacks. *IEEE Transactions on Automatic Control*, 63(7): 2272–2279, 2017.
- Kwon, C., Liu, W., and Hwang, I. Analysis and design of stealthy cyber attacks on unmanned aerial systems. *Journal of Aerospace Information Systems*, 11(8):525–539, 2014.
- Kwon, C., Yantek, S., and Hwang, I. Real-time safety assessment of unmanned aircraft systems against stealthy cyber attacks. *Journal of Aerospace Information Systems*, 13(1):27–45, 2016.
- Lesi, V., Jovanov, I., and Pajic, M. Network scheduling for secure cyber-physical systems. In *2017 IEEE Real-Time Systems Symposium (RTSS)*, pp. 45–55, Dec 2017a. doi: 10.1109/RTSS.2017.00012.
- Lesi, V., Jovanov, I., and Pajic, M. Security-aware scheduling of embedded control tasks. *ACM Trans. Embed. Comput. Syst.*, 16(5s):188:1–188:21, September 2017b. ISSN 1539-9087. doi: 10.1145/3126518. URL <http://doi.acm.org/10.1145/3126518>.
- Lesi, V., Jovanov, I., and Pajic, M. Integrating security in resource-constrained cyber-physical systems. *ACM Trans. Cyber-Phys. Syst.*, 4(3), May 2020. ISSN 2378-962X. doi: 10.1145/3380866. URL <https://doi.org/10.1145/3380866>.
- Li, J., Lee, J. Y., Yang, Y., Sun, J. S., and Tomsovic, K. ConAML: Constrained Adversarial Machine Learning for Cyber-Physical Systems. *arXiv:2003.05631 [cs]*, 2020.
- Miao, F., Pajic, M., and Pappas, G. Stochastic game approach for replay attack detection. In *IEEE 52nd Annual Conference on Decision and Control (CDC)*, pp. 1854–1859, Dec 2013. doi: 10.1109/CDC.2013.6760152.
- Miao, F., Zhu, Q., Pajic, M., and Pappas, G. J. Coding schemes for securing cyber-physical systems against stealthy data injection attacks. *IEEE Transactions on Control of Network Systems*, 4(1):106–117, March 2017. ISSN 2372-2533. doi: 10.1109/TCNS.2016.2573039.
- Mo, Y. and Sinopoli, B. On the performance degradation of cyber-physical systems under stealthy integrity attacks. *IEEE Transactions on Automatic Control*, 61(9):2618–2624, 2015.
- Moosavi-Dezfooli, S.-M., Fawzi, A., and Frossard, P. Deepfool: a simple and accurate method to fool deep neural networks. In *Proceedings of the IEEE conference on computer vision and pattern recognition*, pp. 2574–2582, 2016.
- Navarro, J. A very simple proof of the multivariate chebyshev’s inequality. *Communications in Statistics-Theory and Methods*, 45(12):3458–3463, 2016.
- Pajic, M., Lee, I., and Pappas, G. J. Attack-resilient state estimation for noisy dynamical systems. *IEEE Transactions on Control of Network Systems*, 4(1):82–92, March 2017a. ISSN 2372-2533. doi: 10.1109/TCNS.2016.2607420.
- Pajic, M., Weimer, J., Bezzo, N., Sokolsky, O., Pappas, G. J., and Lee, I. Design and implementation of attack-resilient cyberphysical systems: With a focus on attack-resilient state estimators. *IEEE Control Systems Maga-*

zine, 37(2):66–81, April 2017b. ISSN 1941-000X. doi: 10.1109/MCS.2016.2643239.

Papernot, N., McDaniel, P., Goodfellow, I., Jha, S., Celik, Z. B., and Swami, A. Practical black-box attacks against machine learning. In *Proceedings of the 2017 ACM on Asia conference on computer and communications security*, pp. 506–519, 2017.

Smith, R. S. Covert misappropriation of networked control systems: Presenting a feedback structure. *IEEE Control Systems Magazine*, 35(1):82–92, 2015.

Sui, T., Mo, Y., Marelli, D., Sun, X.-M., and Fu, M. The vulnerability of cyber-physical system under stealthy attacks. *IEEE Transactions on Automatic Control*, 2020.

Szegedy, C., Zaremba, W., Sutskever, I., Bruna, J., Erhan, D., Goodfellow, I., and Fergus, R. Intriguing properties of neural networks. *arXiv preprint arXiv:1312.6199*, 2013.

Teixeira, A., Shames, I., Sandberg, H., and Johansson, K. H. Revealing stealthy attacks in control systems. In *2012 50th Annual Allerton Conference on Communication, Control, and Computing (Allerton)*, pp. 1806–1813. IEEE, 2012.

Tunga, R., Murguia, C., and Ruths, J. Tuning windowed chi-squared detectors for sensor attacks. In *2018 Annual American Control Conference (ACC)*, pp. 1752–1757. IEEE, 2018.

Y. Mo and B. Sinopoli. False data injection attacks in control systems. In *First workshop on Secure Control Systems*, pp. 1–6, 2010.

Yuan, X., He, P., Zhu, Q., and Li, X. Adversarial examples: Attacks and defenses for deep learning. *IEEE transactions on neural networks and learning systems*, 30(9): 2805–2824, 2019.

Zizzo, G., Hankin, C., Maffei, S., and Jones, K. Adversarial Machine Learning Beyond the Image Domain. In *Proceedings of the 56th Annual Design Automation Conference 2019*, pp. 1–4, 2019.